Pergamon

PII: S0146-6380(97)00014-4

Org. Geochem. Vol. 26, No. 5/6, pp. 321–339, 1997

0146-6380/97 $17.00 + 0.00

Thermal cracking of kerogen in open and closed systems: determination of kinetic parameters and stoichiometric coefficients for oil and gas generation

F. BEHAR[1], M. VANDENBROUCKE[1], Y. TANG[2], F. MARQUIS[1] and J. ESPITALIE[1]

[1]Geology–Geochemistry Division, IFP, 1–4 Avenue de Bois Préau, 92506 Rueil-Malmaison Cedex, France and [2]Chevron Petroleum Technology, 1300 Beach Blvd, Box 446, La Habra, CA 90633-046, U.S.A

(Received 29 July 1996; returned to author for revision 18 November 1996; accepted 18 February 1997)

Abstract—The purpose of the study is to compare artificial maturation of kerogens representative of the main types of organic matter (kerogen Types I, II, II-S and III) in open and anhydrous closed pyrolysis systems. The generated compounds are fractionated according to their thermal stability into six chemical classes: C_1, C_2–C_5, C_6–C_{14}, C_{15+} saturates, C_{15+} aromatics and NSOs, which include resins and asphaltenes. In both systems, primary cracking of kerogen can be described by two main reactions: oil generation together with early gas generation followed by late gas production. Mass balances obtained in the two pyrolysis systems are reasonably similar, although some secondary cracking of the NSOs and underestimation of methane potential due to incomplete pyrolysis may occur in the open system. Kinetic parameters of thermal cracking are derived from experiments in the open system using an optimization procedure which determines a unique frequency factor and a weight distribution of chemical classes for a discrete series of activation energies. The resultant frequency factors are checked with those obtained for specific molecular tracers such as n-C_{12}- and n-C_{24}-alkanes generated from kerogens in open and closed systems under isothermal conditions. The results show that using a unique frequency factor as determined by optimization is correct for Type I, II and II-S kerogens. This factor is more questionable, however, when the distribution of activation energies is very broad, such as for Type III coals. Based on this study, a strategy for determination of kinetic parameters on any new source rock sample is proposed. © 1997 Elsevier Science Ltd

Key words—kerogen cracking, kinetic parameters, artificial maturation, open pyrolysis system, closed pyrolysis system

INTRODUCTION

Kerogen is the most abundant component of sedimentary organic matter. As sediments are buried, kerogen undergoes thermal cracking which leads to petroleum generation. Further thermal degradation of kerogen and/or petroleum produces gases. The prediction of both the quantity and quality of oil and gas generated from a given kerogen remains a key problem in petroleum exploration. In natural systems, it is never possible to quantify directly the amount of gas and light hydrocarbons generated because either the volatile compounds have been already expelled or a loss of gas and light oil occurs during sampling. The only way to quantify the complete generation of gas and oil for coals and kerogens is to perform artificial maturation experiments. These may be done at constant or programmed temperature either in an open pyrolysis system swept by an inert gas or in a closed pyrolysis system without effluent sweeping (Solomon *et al.*, 1984; Monthioux *et al.*, 1985; Serio *et al.*, 1987; Espitalié *et al.*, 1988; Horsfield *et al.*, 1989; Monin *et al.*, 1990; Ungerer, 1990; Burnham and Braun, 1990; Behar *et al.*, 1991a; Teerman and Hwang, 1991; Price and Wenger, 1991; Reynolds and Burnham, 1993; Lewan, 1993; Behar *et al.*, 1995).

Kinetic parameters of kerogen cracking are usually determined from experimental data on artificial maturation of kerogen either in open or closed pyrolysis systems in the temperature range of 250–600°C. Assuming that the rate constant dependence with temperature follows an Arrhenius equation, calculations are done through mathematical optimizations of experimental data, which allow the determination of various sets of kinetic parameters for the activation energies (E_a) and frequency factors (A). Very broad ranges for E_a and A values are available in the literature (Ungerer, 1990), leading to a great uncertainty in prediction of the depth of the oil window when extrapolated to geological conditions (Waples *et al.*, 1992). Consequently, the validity of the kinetic parameters obtained by experimental simulation of kerogen degradation depends on the reaction scheme used to describe

kerogen cracking, on the choice of the experimental system for simulating the thermal decomposition of the kerogen and finally on the set of E_a/A values obtained by mathematical optimization procedures.

The aim of the present study is to compare mass balances and kinetic parameters obtained during artificial maturation of kerogen in open and anhydrous closed systems. The following research strategy has been followed:

1. selection of kerogens representative of the main types of organic matter (Types I, II, II-S and III) at the onset of catagenesis in order to follow both oil and gas generation
2. comparison of mass balances obtained in open and closed systems
3. determination in an open system, under non-isothermal conditions, of the frequency factor and the weight distribution of total effluents for discrete steps of activation energies by mathematical optimization (Ungerer and Pelet, 1987; Burnham and Braun, 1990)
4. determination under isothermal conditions, in open and closed systems, of the order and degradation rate for a reaction that produces specific compounds such as *n*-C_{12} and *n*-C_{24} (Tang and Behar, 1995; Behar *et al.*, 1997). The frequency factors obtained for the generation of these two *n*-alkanes will be compared to the one obtained for total effluents through mathematical optimization
5. proposal of a methology for the determination of kinetic parameters for any kerogen.

EXPERIMENTAL

Open system pyrolysis

In order to get a complete mass balance of the pyrolysis products and to derive the kinetic parameters, three different pyrolysis systems were used:

- compositional Rock-Eval pyrolysis for the bulk quantification of the C_1, C_2–C_5, C_6–C_{14} and C_{15+} fractions
- preparative pyrolysis for the quantification of the C_6–C_{14} and the C_{15+} fractions, then the fractionation of the C_{15+} compounds into saturates, aromatics and NSOs
- multi-cold-trap pyrolysis gas chromatography for the quantification of the *n*-alkanes generated under isothermal conditions.

Compositional Rock-Eval pyrolysis. Classical Rock-Eval pyrolysis of source rocks quantifies free petroleum compounds (S_1 peak) already formed and the remaining compounds to be generated by the cracking of kerogen (S_2 peak). A specific Rock-Eval device was used for the present study in order to quantify separately the C_1, C_2–C_5, C_6–C_{14} and C_{15+} bulk fractions in the S_2 peak (Espitalié *et al.*, 1988). Typically, pyrolysis was carried out on 10 mg of kerogen. The pyrolysis chamber was connected to two detectors: a flame ionization detector (FID) and an infra-red detector (IRD) which enabled the specific quantification of methane. For a given sample, three successive pyrolysis runs were needed to obtain the four selected classes. During the first pyrolysis, two traps containing respectively 3 Å and 10 Å molecular sieves were maintained at 50°C in order to retain the C_{6+} compounds; the total fraction C_1–C_5 was split. One aliquot was quantified by the FID, the other was analysed with the IRD. By subtracting the two signals, the separate quantification of the C_1 and the C_2–C_5 fraction (labelled "1") was obtained. Then, during the second pyrolysis, only the trap with the 3 Å molecular sieve was used and heated at 200°C in order to retain the C_{15+} compounds. As for the C_1–C_5 fraction, the C_1–C_{15} compounds were quantified by FID and IRD in order to get the amount of C_1 and C_2–C_{15} (labelled "2"). During the third pyrolysis, there was no trap and thus the total pyrolysate (S_2 peak) was quantified by FID whereas methane was again measured by IRD. The yield of C_6–C_{14} was determined by subtracting fraction "2" from fraction "1". The three independent determinations of the methane provided a check on sampling homogeneity.

For kinetic parameters, we selected four heating rates: 2°C/min, 5°C/min, 10°C/min and 15°C/min. A new version of the Opkin 1 software (Espitalié *et al.*, 1993) was used to determine the frequency factor and the weight distributions of fractions according to increasing activation energies.

Preparative pyrolysis. The preparative pyrolysis device is a cylindrical minifurnace coated with gold to avoid wall effects, as described in previous publications (Behar and Pelet, 1985; Behar *et al.*, 1989). About 20–30 mg of kerogen loaded on a gold rod was introduced into the pyrolysis chamber under an argon flow. After preliminary heating at 300°C for 3 min, the temperature was raised to 600°C at a rate of 25°C/min, with a temperature program similar to that of classical Rock-Eval pyrolysis. Effluents were condensed, with the carrier gas, in a trap cooled with liquid nitrogen. The pyrolysate was then recovered by the addition of solvent at room temperature, resulting in argon elimination and loss of C_1–C_5 products. Two pyrolysis experiments were needed for the quantification of the C_{6+} fraction. The first pyrolysate was recovered with *n*-pentane and injected as such into a gas chromatograph for the quantification of the C_6–C_{14} fraction by the FID, previously calibrated with an external standard (saturated C_{15}–C_{25} distillation cut). The second pyrolysate was recovered in dichloromethane. The C_{15+} fraction quantified by weighing was

fractionated by liquid chromatography into saturates, aromatics and NSO compounds.

Multi-cold-trap pyrolysis gas chromatography (MCTP–GC). The MCTP–GC instrument permits pyrolyses in an open system under isothermal conditions (Tang and Stauffer, 1994a,b). About 6 mg of dry kerogen was loaded into a quartz tube (20 mm length, 2 mm ID) plugged on one side with quartz wool and placed in a pyroprobe with a thermocouple in contact with the sample. After a short purge cycle, the temperature of the pyroprobe was raised to 300°C for 6 min and any free hydrocarbon was vented through a secondary valve. This valve was then rotated and the pyrolysis carrier gas (30 ml/min helium) was diverted to liquid nitrogen-filled cold traps. As the sample was pyrolysed, the 22 port valve advanced automatically at certain preset temperature or time points in order to capture the pyrolysis products in the individual traps. When the pyrolysis was finished, each trap contained a thermal or time "slice" of the pyrolysate, frozen and sealed at liquid nitrogen temperature. Each trap was then sequentially drained of liquid nitrogen, switched to the GC and ballistically heated to 300°C in order to send the sample to the GC column for quantitative analysis.

Closed system pyrolysis

Isothermal pyrolysis was carried out at temperatures between 300 and 500°C during time intervals ranging from 1 to 72 h. All pyrolysis experiments were performed in gold tube reactors (9 mm OD, L = 60 mm). Typically, 400 mg of kerogen was loaded into the tubes for C_{6+} quantitation. A separate set of experiments was carried out using 50 mg, in proportionally smaller tubes, for precise gas measurements. The loaded tubes were flushed with argon several times to ensure complete removal of air; the other end of the gold tube was then welded under argon. The tubes were then placed in stainless steel cells next to a thermocouple in a similar empty tube, providing control of the temperature to ±1°C. The cells were placed in a furnace preheated at the chosen isothermal temperature (the heat-up time for a sample being typically ~15 min) and kept at a pressure of 12 MPa during the experiment. Pyrolysis time was measured from the point when the desired isothermal temperature was reached: this was recorded and stored on a computer. At the end of the desired reaction time the cells were taken out and cooled to 150°C with compressed air then immersed in a water bath.

The products were separated into several fractions using the procedure of Behar *et al.* (1989) and Behar *et al.* (1991a). For the C_{6+} fraction recovery, the gold tube was immersed in dichloromethane (DCM) and pierced with a needle. The tube was then cut open and the solvent and tube contents were removed and transferred into an agate dish filled with DCM. The sample, soaked in DCM, was ground for 5 min. The products (together with gold pieces) were then extracted under reflux in DCM for 1 h and filtered into a tared flask, allowing quantitation of the total solution by weighing. For the two Type III kerogens, due to high matrix retention preventing efficient solvent access, the insoluble residue was extracted with a mixture of $CHCl_3$/MeOH/HCl and filtered. The insoluble residue was dried, weighed and stored under an argon atmosphere. It was then submitted to Rock-Eval pyrolysis in order to quantify the residual S_1 if any (Type III) and the residual S_2, to be used in the mass balance calculation.

A weighed aliquot of the DCM extract was used for the quantitation of the C_{15+} fraction by evaporation and weighing, then fractionated by microcolumn liquid chromatography (Behar *et al.*, 1989) into saturates (SAT), aromatics (ARO) and NSOs. Another aliquot was taken for determining the amount of asphaltenes (ASP) by adding *n*-heptane to the evaporated extract in order to control the beginning of secondary cracking. A third aliquot was injected into a gas chromatograph for quantification of the C_6–C_{14} fraction, using the same procedure as described previously for preparative pyrolysis. However, the quantitative measurement of the C_6–C_{14} fraction was often hampered by the partial evaporation of C_6–C_9 compounds during product work up.

The gases obtained separately in the smaller gold tubes were measured quantitatively using a vacuum line connected to a Toepler pump. Molecular characterization and relative quantification of the generated gases were performed by gas chromatography. Individual gas amounts were then lumped into C_1, C_2–C_5 and non-hydrocarbons (CO_2 and H_2S).

Mass balance and gas/oil ratio (GOR) calculations. The initial hydrogen index (HI_o) can be compared to the calculated hydrogen index of the studied kerogen, for any pyrolysis experiment in a closed system, resulting from the mass balance as follows:

$$HI_c = (C_1) + (C_2 - C_5) + (C_6 - C_{14}) + (C_{15+}) + (S_{1r}/C_o) \times (W_r/W_o) + (S_{2r}/C_o) \times (W_r/W_o)$$

where HI_o is the measured hydrogen index of the initial kerogen, HI_c is the calculated hydrogen index for any experiment (in mg/g of initial carbon), C_o is the organic carbon content, W_o is the weight of the initial kerogen, (C_1), $(C_2$–$C_5)$, $(C_6$–$C_{14})$ and (C_{15+}) are the amounts (mg/g of initial organic carbon) of petroleum fractions generated, S_{2r} is the measured S_2 peak (in mg/g residual kerogen), S_{1r} is the S_1 peak (mg/g residual kerogen, exists for kerogen Type III only) and W_r is the weight of the residual kerogen: HI_c should be equal to HI_o but due to the analytical uncertainties in weighing and Rock-Eval

data, this calculation cannot be more than a mere verification of consistency of experimental results. However, systematic deviations can be explained as discussed in the Results and Discussion section.

The mass gas/oil ratio $(GOR)_m$ is calculated as follows:

$$GOR_m = ((C_1) + (C_2 - C_5))/((C_6 - C_{14}) + (C_{15+}))$$

In order to express this ratio volumetrically (GOR_v, in m^3 of gas per m^3 of oil), the following calculations were done.

Estimating the C_{6+} density to be 0.9 g/cm^3 or 900 g/l, the oil volume is:

$$((C_6 - C_{14}) + (C_{15+}))/900$$

If MW is the average molecular weight of the C_2–C_5 fraction, and all gases are assumed to be ideal, i.e. occupying 22.4 l/mol in standard conditions, then:

$$GOR_v = 900 \times 22.4 \times ((C_1)/16 + (C_2 - C_5)/MW)/((C_6 - C_{14}) + (C_{15+})) \text{ in } m^3/m^3$$

SAMPLES

A shale from the Green River Formation (Eocene) containing Type I kerogen, a Toarcian shale from the Paris Basin (Toarcian) of Type II kerogen, a Monterey Shale (Miocene) with Type II-S kerogen and two coals from, respectively, the Mahakam Delta (Miocene) and the North Sea (Dogger) representing Type III organic matter were selected at diagenetic levels corresponding to the beginning of the oil window. For both shales and coals, kerogens were prepared by HF/HCl digestion according to the standard procedure described by Durand and Nicaise (1980), then extracted with dichloromethane. Kerogen isolation is necessary to avoid any interference with minerals, the chemical properties of which are drastically modified compared with those under geological conditions because of the high temperatures needed for pyrolysis (Espitalié *et al.*, 1984). Typing and maturity of these reference kerogens were determined by elemental analysis, Rock-Eval pyrolysis, vitrinite reflectance and product distributions in the GC traces of C_{6+} pyrolysates from preparative pyrolysis. These analyses are given in Table 1 and Fig. 1. All samples have a maturation stage corresponding to the very end of diagenesis, except the North Sea Type III sample which is at the beginning of the catagenesis stage.

GC traces of total hydrocarbons from pyrolysates show clear structural differences between individual kerogens (Fig. 1). Type I is dominated by *n*-alkane/alkenes showing a bimodal distribution in a broad carbon range (*n*-C_{10} to *n*-C_{30}). Type II contains more *iso*-alkane/alkenes and pristene than Type I with a regularly decreasing carbon distribution. Type II-S has a distribution fairly similar to Type II but with a large number of supplementary peaks due to sulfur-containing compounds as evidenced by GC–MS. Type III, similarly to Type I, shows a flat distribution for *n*-alkane/alkenes, here without strong odd/even predominance in opposition to other similar coals but with major peaks from aromatics in the C_6–C_{10} range. A difference appears in the ratio between the saturated and aromatic fractions generated by the two Type III samples: the Mahakam coal generates more *n*-alkane/alkenes and pristene whereas aromatics are major products in the North Sea coal. The small difference in maturity cannot explain such a different composition. This might be due either to different higher plant chemical composition, linked to their different geological ages, or else to different climatic conditions leading to different vegetal species and preservation conditions. This is the reason why both Type III kerogens were selected for the present study.

RESULTS AND DISCUSSION

Comparison of mass balances

Open system pyrolysis. Compositional Rock-Eval pyrolysis, which separates effluents into four classes according to their carbon range, was used for the five samples under study. Table 2 shows increasing steps of activation energy, i.e. increasing temperature, for the generated fraction of the total hydrogen index, separated into C_1, C_2–C_5, C_6–C_{14} and C_{15+} compounds. The evolution of mass balances shows, for all kerogens, two main reactions: the

Table 1. Geochemical characterization of the studied kerogens: Rock-Eval parameters (T_{max} and HI), vitrinite reflectance (R_o) and atomic ratios H/C and O/C show that the selected samples are at the beginning of the oil window

Type	Origin	T_{max} (°C)	HI (mg/g C)	R_o (%)	organic C (wt%)	H/C	O/C
I	Green River Fm	438	918	nd	66.88	1.55	0.081
II	Paris Basin	419	600	0.55	55.33	1.27	0.145
II-S	Monterey	403	560	nd	63.29	1.26	0.102
III	Mahakam Delta	419	194	0.57	76.14	0.84	0.152
III	North Sea	431	212	0.62	78.84	0.80	0.120

nd:.

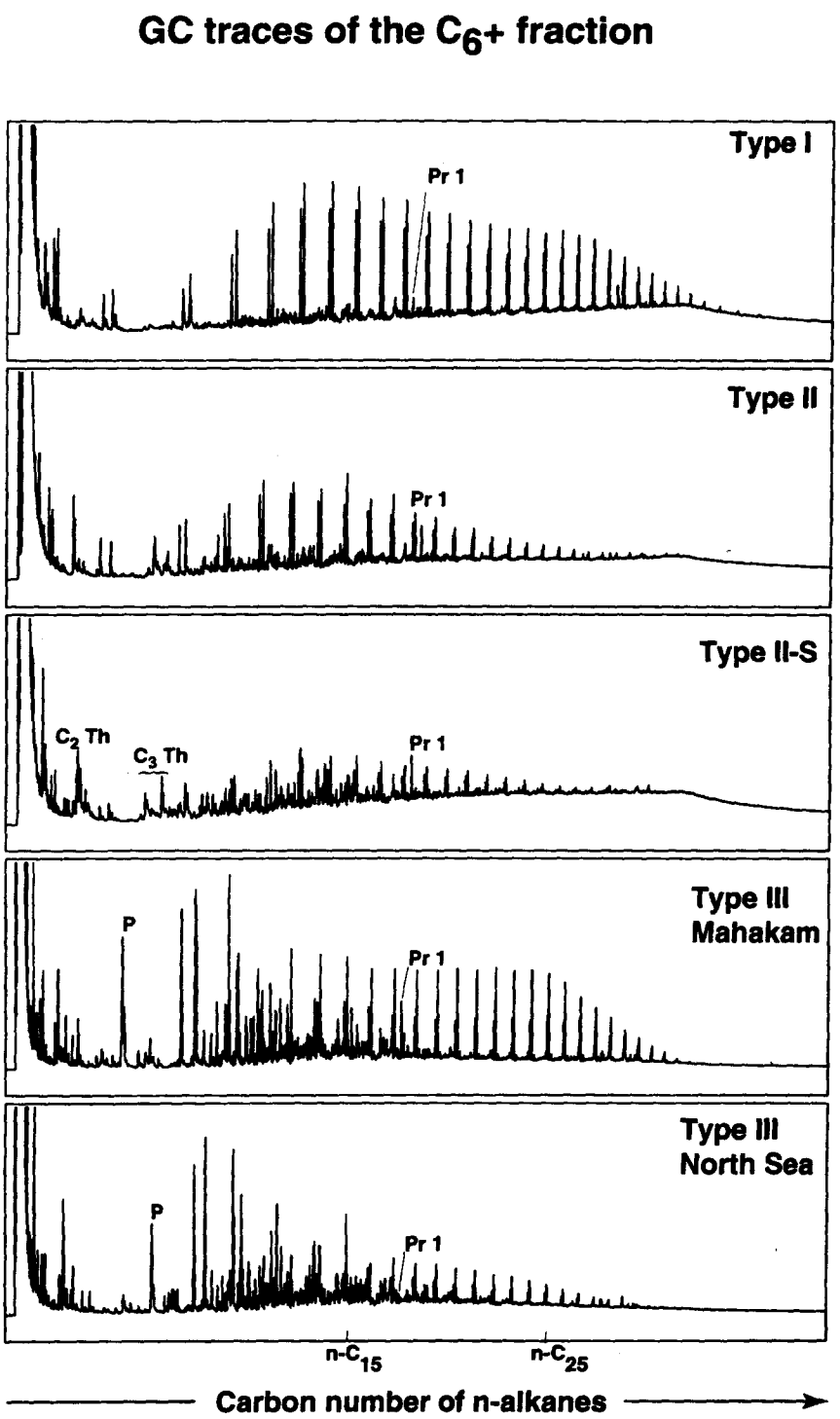

Fig. 1. GC traces of the total C_{6+} fraction recovered during preparative pyrolysis of the initial kerogens under study. Carbon number distribution of alkane–alkene doublets, and the relative abundance of low molecular weight aromatic compounds, are characteristic of kerogen types (see text and among others Larter, 1984). Prl is pristene-1, C_2Th and C_3Th are alkylated thiophenes and P is phenol.

Table 2. Absolute yields (mg/g C) of the C_1, C_2–C_5, C_6–C_{14} and C_{15+} compounds generated during compositional Rock-Eval pyrolysis for increasing steps of activation energy, i.e. increasing temperature

E (kcal/mol)	Type I					Type II					Type II-S					Type III Mahakam					Type III North Sea				
	C_1	C_2–C_5	C_6–C_{14}	C_{15+}	HI	C_1	C_2–C_5	C_6–C_{14}	C_{15+}	HI	C_1	C_2–C_5	C_6–C_{14}	C_{15+}	HI	C_1	C_2–C_5	C_6–C_{14}	C_{15+}	HI	C_1	C_2–C_5	C_6–C_{14}	C_{15+}	HI
44	0.0	0.0	0.0	0.0	0.0	0.0	0.0	0.0	0.0	0.0	0.3	0.5	2.7	5.2	8.7	0.0	0.0	0.0	0.0	0.0	0.0	0.0	0.0	0.0	0.0
46	0.0	0.0	0.0	0.0	0.0	0.0	0.1	0.6	0.7	1.4	1.1	2.8	7.8	46.0	57.7	0.0	0.0	0.0	0.0	0.0	0.0	0.0	0.0	0.0	0.0
48	0.0	0.0	0.0	0.0	0.0	0.3	0.8	3.1	6.5	10.7	1.8	9.4	24.5	151.4	187.1	0.0	0.0	0.0	0.0	0.0	0.0	0.0	0.0	0.0	0.0
50	0.0	0.0	0.0	0.0	0.0	0.9	4.6	7.9	53.9	67.3	2.1	6.9	20.6	158.7	188.3	0.0	0.2	0.0	1.6	1.8	0.0	0.0	0.0	0.0	0.0
52	0.4	3.5	8.1	0.0	12.0	2.0	12.1	14.1	157.3	185.4	2.1	11.8	23.6	39.1	76.6	0.0	0.5	0.4	3.3	4.2	0.0	0.0	0.0	0.0	0.0
54	6.3	68.6	83.0	738.7	896.6	2.9	12.4	20.2	250.4	285.9	3.8	8.5	3.7	6.6	22.6	0.3	1.1	1.5	7.9	10.8	0.0	0.0	0.4	0.8	1.2
56	3.1	0.0	0.0	0.0	3.1	2.9	11.3	7.3	7.4	29.0	4.9	2.4	0.0	0.0	7.3	0.9	3.0	2.6	33.3	39.8	0.1	0.4	1.2	24.8	26.5
58	2.0	0.0	0.0	0.0	2.0	3.6	4.6	0.4	1.4	10.0	4.2	1.3	0.0	0.0	5.5	2.0	5.3	7.8	40.8	55.9	1.0	3.0	4.2	72.6	80.8
60	1.6	0.0	0.0	0.0	1.6	2.5	2.0	0.0	0.0	4.5	4.6	0.3	0.0	0.0	4.9	3.5	6.7	5.1	20.5	35.8	2.9	6.2	7.4	30.7	47.2
62	1.3	0.0	0.0	0.0	1.3	2.0	1.2	0.0	0.0	3.2	0.9	0.0	0.0	0.0	0.9	4.4	3.9	3.5	6.6	18.4	4.0	6.5	3.8	7.1	21.4
64	1.3	0.0	0.0	0.0	1.3	1.4	0.7	0.0	0.0	2.1	0.5	0.0	0.0	0.0	0.5	5.0	1.6	1.4	2.1	10.0	4.8	4.7	0.3	1.6	11.4
66	0.4	0.0	0.0	0.0	0.4	0.3	0.3	0.0	0.0	0.6	0.1	0.0	0.0	0.0	0.1	5.0	0.9	0.7	0.4	7.0	4.9	2.5	0.0	0.0	7.4
68	0.0	0.0	0.0	0.0	0.0	0.0	0.1	0.0	0.0	0.1	0.0	0.0	0.0	0.0	0.0	4.8	0.4	0.0	0.0	5.2	4.2	1.2	0.0	0.0	5.4
70	0.0	0.0	0.0	0.0	0.0	0.0	0.0	0.0	0.0	0.0	0.0	0.0	0.0	0.0	0.0	4.0	0.0	0.0	0.0	4.0	4.1	1.5	0.0	0.0	5.6
72	0.0	0.0	0.0	0.0	0.0	0.0	0.0	0.0	0.0	0.0	0.0	0.0	0.0	0.0	0.0	0.7	0.0	0.0	0.0	0.7	3.9	0.2	0.0	0.0	4.1
74	0.0	0.0	0.0	0.0	0.0	0.0	0.0	0.0	0.0	0.0	0.0	0.0	0.0	0.0	0.0	0.0	0.0	0.0	0.0	0.0	1.0	0.0	0.0	0.0	1.0
Total	16.4	72.1	91.1	738.7	918.3	18.8	50.2	53.7	477.6	600.3	26.4	43.9	82.9	407.0	560.2	30.6	23.6	23.0	116.4	193.6	30.9	26.2	17.3	137.6	212.0
	$A = 7.4 \times 10^{13}$ (s^{-1})					$A = 1.6 \times 10^{14}$ (s^{-1})					$A = 2.5 \times 10^{13}$ (s^{-1})					$A = 3.0 \times 10^{15}$ (s^{-1})					$A = 3.1 \times 10^{15}$ (s^{-1})				

first with quasi-simultaneous generation of C_2–C_5, C_6–C_{14} and C_{15+} compounds plus some C_1 (oil generation), then a second corresponding to C_1 (dry gas) generation. However, the timing of these reactions cannot be directly compared on the *E* values as the pre-exponential factors, discussed later, are different. Table 3 gives the corresponding balance of the four classes in the total hydrogen index in mg/g C and in %. In all samples, the effluent distribution is dominated by the C_{15+} fraction which represents 60 to 80 wt% of the total pyrolysate. For the Type I, II and II-S kerogens, hydrocarbon gases (C_1–C_5) do not exceed 12 wt% of the pyrolysate, while they represent more than 25 wt% for the two coals.

To account for the different thermal stabilities of generated compounds in the C_{6+} range, a separation according to their chemical structure and not only their molecular weight is necessary. Preparative pyrolysis permitted recovery of the C_{6+} products in order to quantify the C_6–C_{14} and the C_{15+} fractions and to determine the absolute amounts of saturates, aromatics and NSO compounds in the C_{15+} fraction. Results (Table 4) show that similar yields (mg/g C) were obtained for the C_6–C_{14} and C_{15+} fractions recovered by preparative pyrolysis and Rock-Eval pyrolysis. This means that the cut-off according to carbon numbers obtained by the trapping of effluents during Rock-Eval pyrolysis does not depend on the chemical composition of the pyrolysate.

The absolute amounts and relative distribution of the C_{15+} saturates, aromatics and NSOs, which represent the major part of the S_2 peak of the Rock-Eval, are given in Table 5. Differences between saturated and aromatic hydrocarbons in the C_{15+} pyrolysates are observed, not only between different kerogen types but even for the Mahakam and North Sea coals: the data confirm the qualitative difference suggested by the GC of their C_{6+} fraction. The same is true with the present GRS sample which generates an amount of saturates very close to other Type I reference samples previously studied, but much more aromatics and NSOs. These results show that Type I and Mahakam Type III generate hydrocarbons rich in saturates, whereas Types II and II-S generate mainly aromatics and naphthenoaromatics, with probably a large contribution of sulfur-containing compounds to the aromatic fraction for Type II-S. They show also that the NSOs, even for the Type I kerogen studied here, are major compounds in the C_{15+} pyrolysate. This suggests that in the open system a large part of the heavy compounds generated during kerogen cracking may be vaporized and swept away from the pyrolysis chamber by the carrier gas. It is generally believed that the hydrogen indices represent a yield of hydrocarbons released during primary cracking. Our results demonstrate

Table 3. Compositional Rock-Eval mass balances for the selected kerogens

	C_1		C_2–C_5		C_6–C_{14}		C_{15+}		HI
Kerogen	mg/g C	%	mg/g C	%	mg/g C	%	mg/g C	%	mg/g C
Type I	16	2	72	8	91	10	739	80	918
Type II	19	3	50	8	54	9	477	80	600
Type II-S	26	4	44	8	83	15	407	73	560
Type III Mahakam	31	16	24	13	23	10	116	61	194
Type III North Sea	31	15	26	12	17	8	138	65	212

Table 4. Comparison of the yields of C_6–C_{14} and C_{15+} fractions recovered in Rock-Eval and preparative pyrolysis (amounts are given in mg/g C)

	Rock-Eval pyrolysis		Preparative pyrolysis	
Kerogen	C_6–C_{14}	C_{15+}	C_6–C_{14}	C_{15+}
Type I	91	739	95	750
Type II	54	477	63	488
Type II-S	83	407	75	450
Type III Mahakam	23	116	27	106
Type III North Sea	17	138	18	133

Table 5. Fractionation by liquid chromatography of the C_{15+} fraction recovered during preparative pyrolysis into saturates (SAT), aromatics (ARO) and NSO compounds (NSO)

		SAT	ARO	NSO	HC	SAT	ARO	NSO	ARO/SAT
Kerogen	C_{15+} (mg/g C)	(mg/g C)				(wt%)			
Type I	750	172	270	308	442	23	36	41	1.6
Type II	488	33	136	319	169	7	28	65	4.1
Type II-S	450	33	165	252	198	7	37	56	5.0
Type III Mahakam	106	13	16	77	29	12	15	73	1.2
Type III North Sea	133	9	25	98	34	7	19	74	2.8

Table 6. Real hydrocarbon mass balances (mg/g C) and gas/oil ratio (GOR) calculation: HC corresponds to the effluents without the contribution of the NSO compounds, HI is the hydrogen index, *v/v* is the volume/volume ratio

Kerogen	C_1	C_2–C_5	C_6–C_{14}	C_{15+} SAT + ARO	Total HC	GOR *v/v*	HC/HI
Type I	16	72	91	442	621	129	0.68
Type II	19	50	54	169	292	258	0.49
Type II-S	26	44	83	198	351	222	0.63
Type III Mahakam	31	24	23	29	107	1037	0.55
Type III North Sea	31	26	17	34	108	1108	0.51

that in fact the pyrolysate comprises a complex mixture dominated by polar compounds. The mass balances obtained for the real hydrocarbon distributions and the resulting GORs are given in Table 6.

Type I kerogen generates the highest absolute and relative amount of hydrocarbons. For the other kerogens the hydrocarbon potential represents around half of the total hydrogen indices. Surprisingly, the Type II-S kerogen has the highest proportion of hydrocarbons although this type of organic matter is well known to generate a lot of heavy compounds. It could be due partly to the contribution of sulfur-containing compounds which are separated together with true aromatic hydrocarbons in the C_{6+} fraction and partly to early secondary cracking of NSOs before effluent sweeping by the carrier gas. For Type III coals gases are slightly greater than liquid hydrocarbons, leading to a GOR above 1000 whereas this ratio does not exceed 260 for the Type I, II and II-S kerogens.

We have analysed the changes in chemical composition of the C_{6+} pyrolysate by carrying out preparative pyrolyses with different final temperatures, 475, 500, 530 and 600°C (Fig. 2), on other reference samples (Types I, II and III; Lerat, unpublished results). Results show that there is no significant change in the distribution of the C_{6+} effluents with increasing pyrolysis temperatures in the open system. This means that the C_{15+} class

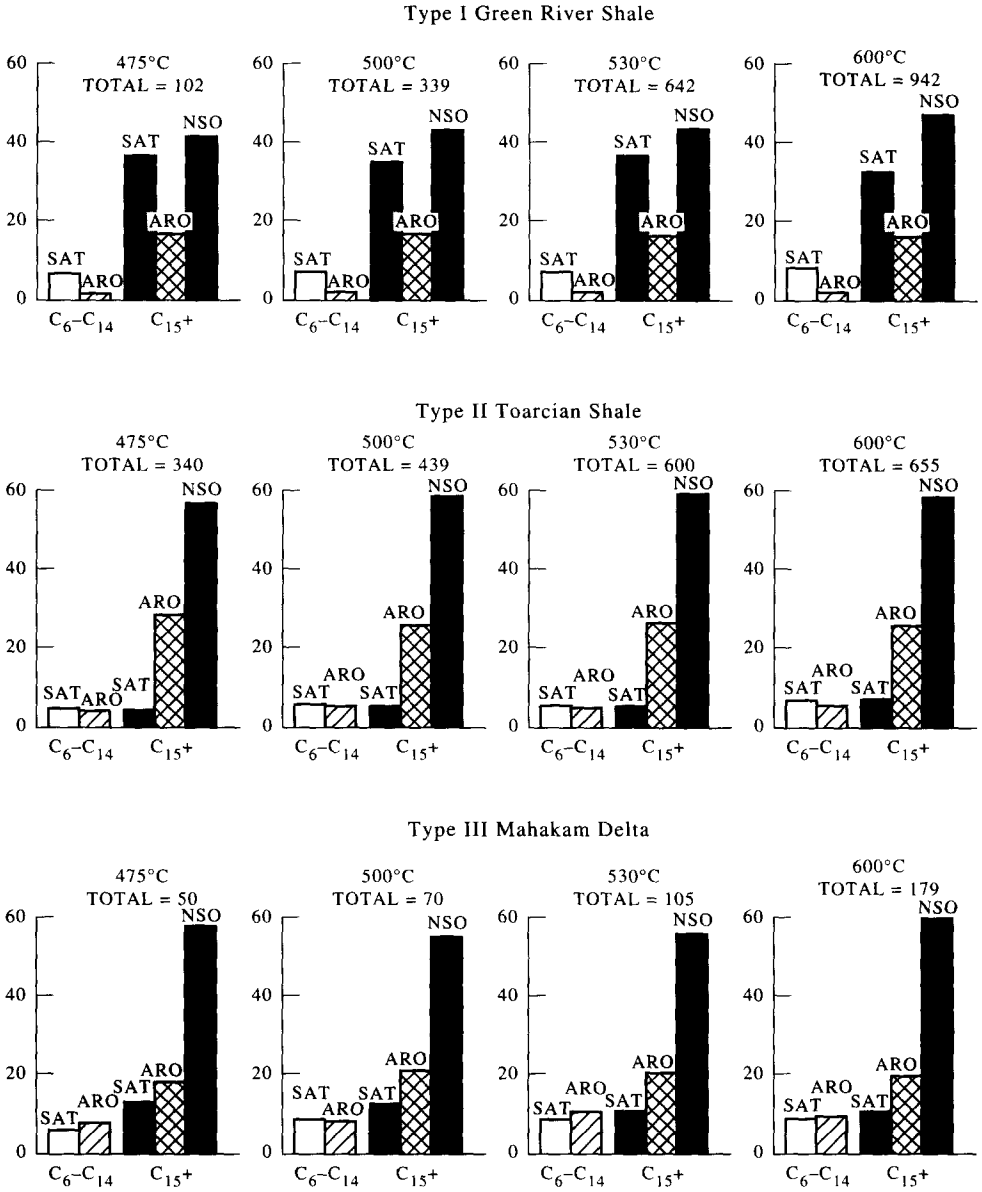

Fig. 2. Relative distribution (%) of the C_{6+} fraction recovered at various final temperatures during preparative pyrolysis of some reference Type I, II and III kerogens (Lerat, IFP unpublished results). Almost no change is observed in the relative proportion of fractions whatever the temperature, although the total amount in mg/g C is multiplied by a factor of at least 2.

given from compositional Rock-Eval pyrolysis can be split into saturates, aromatics and NSOs according to the proportions given in Table 6. Consequently, the pyrolysis products generated from primary cracking in this non-isothermal open system can be described by six chemical classes: C_1, C_2–C_5, C_6–C_{14}, C_{15+} saturates, aromatics and NSOs for any activation energy step.

Closed system pyrolysis. The mass balances obtained for the five kerogens pyrolysed in selected temperature/time conditions are given in Table 7. The sum of the total effluents plus the non-hydrocarbon gases provides by difference the amount of insoluble residue which cannot be recovered quantitatively by filtration. With the residual petroleum potential of this insoluble residue S_{2r} being determined by Rock-Eval pyrolysis, it was possible to calculate the effluent balance HI_c and the transformation ratio $TR = S_{2r}/S_{2o}$ in each experiment, as explained in the Experimental section. We have not included the non-hydrocarbon gases in this balance calculation in order to make a direct comparison with the total hydrogen indices HI_o obtained by classical Rock-Eval pyrolysis in the open system.

Table 7. Primary cracking of kerogen in closed system pyrolysis: mass balances, absolute amounts of saturates (SAT), aromatics (ARO) and NSO compounds (NSO) in the C_{15+} fraction, evaluation of the total effluents without the contribution of the non-hydrocarbon gases ($H_2S + CO_2$), estimation of the residual kerogen potential (S_{2r}) by Rock-Eval pyrolysis, evaluation of the total hydrogen index (HI_c) and calculation of the transformation ratio (TR). All figures are in mg/gC except Residual kerogen proportion and TR which are weight ratios

Sample	T (°C)	t (h)	C_1	C_2–C_5	C_6–C_{14}	C_{15+} extract				Total HC effluents	Non-HC gases	Residual Kerogen		HI_c	TR
						SAT	ARO	NSO	Total			proportion	S_{2r}		
	300	24	1	0	9	10	34	80	124	134	9	0.89	557	576	0.09
	325	24	7	13	30	42	152	390	584	634	25	0.56			
	350	1	1	0	15	10	45	137	192	208	12	0.85	540	897	0.12
	350	2	1	1	21	23	82	245	350	373	14	0.74	450	872	0.27
	350	3	nd	nd	32	38	122	401	561	nd	nd	nd	nd	nd	nd
Type I	350	6	nd	nd	44	51	161	536	748	nd	nd	nd	nd	nd	nd
	350	9	nd	nd	50	63	178	601	842	nd	nd	nd	nd	nd	nd
	350	**15**	**7**	**13**	**68**	**85**	**229**	**640**	**954**	**1047**	**35**	**0.28**	**50**	**1065**	**0.92**
	350	24	8	24	90	125	228	502	855	977	45	0.32	29	985	0.95
	375	15	19	65	133	161	211	238	610	827	129	0.41	14	836	0.98
	300	24	3	4	7	8	61	272	341	355	83	0.75	263	701	0.21
	325	24	5	13	20	24	109	327	460	498	112	0.66	104	623	0.69
	350	1	4	7	10	14	71	354	439	460	94	0.69	207	719	0.38
	350	**2**	**5**	**10**	**14**	**16**	**92**	**350**	**458**	**487**	**99**	**0.68**	**165**	**689**	**0.50**
	350	3	7	15	18	23	94	338	455	495	105	0.67	136	659	0.59
Type II	350	6	9	21	29	32	108	315	455	514	117	0.65	83	612	0.75
	350	9	11	26	37	37	120	293	450	524	129	0.64	71	606	0.79
	350	15	11	30	45	40	122	271	433	519	129	0.64	56	584	0.83
	350	24	12	45	60	55	127	258	440	557	128	0.62	29	589	0.91
	375	15	25	84	83	69	137	199	405	597	189	0.57	7	604	0.98
	300	2	1	3	28	7	55	364	426	458	40	0.67	207	678	0.38
	300	24	3	5	60	15	112	400	527	595	64	0.57	154	734	0.54
	325	1	3	3	47	11	60	397	468	521	87	0.66	187	745	0.44
	325	**3**	**5**	**5**	**59**	**15**	**96**	**396**	**507**	**576**	**94**	**0.63**	**147**	**743**	**0.56**
Type II-S	325	9	6	11	70	20	157	307	484	571	115	0.62	91	673	0.73
	325	15	8	15	81	25	157	319	501	605	118	0.60	78	690	0.77
	325	24	9	20	89	32	160	278	470	588	128	0.60	62	656	0.81
	325	48	12	32	93	36	134	243	413	550	129	0.62	39	598	0.88
	350	24	18	46	111	37	116	170	323	498	150	0.64	29	532	0.91
	300	24	2	2	10	3	4	34	41	55	65	0.91	63	154	0.56
	325	24	3	3	15	5	6	39	50	71	96	0.87	47	143	0.67
	350	**1**	**3**	**4**	**13**	**4**	**5**	**58**	**68**	**88**	**71**	**0.38**	**52**	**163**	**0.64**
	350	2	3	4	13	5	5	55	65	85	73	0.88	53	161	0.64
Type III	350	3	3	5	15	5	5	54	65	88	82	0.87	50	159	0.65
Mahakam	350	9	4	7	19	7	5	40	53	83	90	0.87	37	136	0.75
	350	15	5	7	21	7	6	36	49	83	101	0.86	36	135	0.75
	350	24	6	7	21	8	6	30	44	78	115	0.85	30	122	0.79
	375	24	13	15	21	7	4	25	36	85	127	0.84	21	113	0.86
	300	24	1	1	8	2	4	42	48	58	23	0.94	95	187	0.43
	325	24	1	1	14	2	7	50	59	75	27	0.92	68	172	0.59
	350	1	1	1	10	2	6	57	65	77	27	0.92	75	185	0.55
Type III	350	2	2	2	13	2	8	58	68	84	31	0.91	68	183	0.59
North Sea	**350**	**3**	**3**	**2**	**14**	**3**	**9**	**60**	**72**	**91**	**33**	**0.91**	**66**	**180**	**0.60**
	350	9	4	4	19	4	11	57	72	100	37	0.90	53	176	0.68
	350	24	6	8	25	6	12	55	73	112	43	0.88	38	166	0.77
	375	3	nd	nd	25	6	11	49	66	nd	nd	nd	29	nd	0.83

Unfortunately, only a few insoluble residues could be recovered for some Type I experiments due to difficulties in filtering the dichloromethane solution, thus some results are lacking for this kerogen (Table 7).

As in open system pyrolysis, Type I kerogen generates the largest amount of extractable products, followed by the Type II-S and II samples, the Type III samples having the lowest yield. For all the samples, the pyrolysis products are dominated by the NSO compounds. At their maximum production, they represent from 61 wt% (Type I kerogen) to 84 wt% (Type II-S kerogen) of the total effluents whereas in open system pyrolysis, they did not exceed 51 wt% of the hydrogen indices. The maximum asphaltene production in the NSOs occurs usually at the maximum generation of the total C_{15+} extract, i.e. at 350°C/15 h for the Type I, 350°C/2 h for the Type II, 325°C/3 h for the Type II-S and 350°C/1 h and 3 h for the Type III Mahakam and North Sea samples, respectively. As these asphaltenes are the least stable chemical class among the pyrolysis effluents (Behar *et al.*, 1991b), this means that secondary cracking is very limited before the maximum generation of the C_{15+} fraction. For Type II-S there is a small delay between maximum production of asphaltenes and maximum of the C_{15+}, due to early secondary cracking of

heavy compounds because of their richness in weak sulfur bonds. Light hydrocarbon gases and the C_6–C_{14} fraction are already produced at the onset of primary cracking. Their yield increases greatly when both resins and asphaltenes begin to degrade. Except for the Type II-S kerogen, in which the aromatic fraction contains a large proportion of sulfur-containing compounds (Tomic *et al.*, 1995), the C_{15+} aromatics are not measurably degraded at 350°C/24 h. This shows that even in a closed system coke formation from aromatics is not a straightforward reaction.

In terms of total hydrocarbon balance, for the Type I, II and II-S kerogens, the maximum values of HI_c (measured in the closed system) are always higher than those of HI_o of the open system pyrolysis. However, for the Type I sample, at low severity, the balance of HI_c is lower than the HI_o of the initial sample, probably due to NSO losses during residue filtration. The difference may be explained, as discussed later, by the secondary cracking of some NSOs before effluent sweeping in the open system. The part of NSOs transformed into coke is thus not taken into account in the classical hydrogen index HI_o. For the two Type III kerogens it was not possible in any experiment to reach the hydrogen index HI_o of the initial sample. This may be explained by (i) an early polycondensation in the closed system of aromatic structures leading to coke formation or (ii) trapping of the generated products inside the kerogen network. Because, for all the samples, the yield of the aromatics increases with severity and starts to decrease only when a large part of the NSOs has already been degraded, it seems that rapid coke formation from the aromatics is unlikely. From previous works (Given, 1984; Behar and Vandenbroucke, 1988; Derbyshire *et al.*, 1989) it was concluded that the structural network of coals has a very high trapping efficiency, which increases with maturity. Due to the difficulty of extracting the Type III kerogens (we had to use a mixture of dichloromethane and hydrochloric acid), it is probable that during pyrolysis the kerogen network is reorganized and retains the generated products, leading to an underestimation of the total pyrolysate yield.

After the maximum balance HI_c has been reached, a systematic decrease of this parameter is observed for all the samples with increasing maturity. This can be related to the strong decrease of the NSOs which, upon cracking, produce a large amount of refractory insoluble residue (Behar *et al.*, 1991b) that is no longer oil prone. As this refractory residue is recovered together with the remaining kerogen, the S_2 value obtained on the total insoluble fraction will be underestimated. This explains also the discrepancy observed between the transformation ratio (TR in Table 7) and the estimated proportion of insoluble residue, which hardly decreases even for very high TR values. Finally, the values of the TR increase, as expected, with maturity. However, this parameter is not an absolute maturity scale: it depends directly on the maturity stage of the initial kerogen. For example, for the same pyrolysis conditions, the North Sea sample shows a lower TR than the Mahakam one, due to its higher initial maturity.

Comparison of effluent balance in open and closed pyrolysis systems. In both open and closed systems, primary cracking of kerogens can be described by two main reactions:

$$\text{kerogen 1} \longrightarrow \text{Gas 1} + C_{6+} \text{ products} + \text{kerogen 2} \quad (1)$$

$$\text{kerogen 2} \longrightarrow \text{Gas 2} + \text{dead kerogen} \quad (2)$$

The mass balances obtained in the open system (Table 3) correspond to the complete transformation of the initial kerogen by these two reactions. In order to compare these mass balances to those of the closed system experiments, it is necessary to obtain the mass balances in the closed system for the total transformation in each separate reaction and then calculate the sum of mass balances. Unfortunately, results presented in Table 7 have shown that, in closed system experiments, there is quite a large overlap between primary cracking of kerogen and secondary cracking of NSOs. Thus, in order to calculate the mass balance of the first reaction without secondary cracking for a TR equal to 100%, we have selected the conditions for which we have obtained both the maximum of NSOs and total C_{15+} fraction. These conditions are fulfilled at 350°C/15 h for the Type I, 350°C/2 h for the Type II and 350°C/1 h and 350°C/3 h for the Mahakam and the North Sea samples, respectively. For the Type II-S sample, we have selected the experiment at 325°C/3 h for which the maximum of the C_{15+} fraction was reached. For these five experiments, the relative proportions of the six classes C_1, C_2–C_5, C_6–C_{14}, C_{15+} saturates, C_{15+} aromatics and NSOs in the pyrolysate can be calculated. Based on the constant composition of the C_{6+} fraction observed at any step of the first reaction in the open system (Fig. 2), we will assume that in the closed system the remaining kerogen, after the maximum C_{15+} production, generates the same proportion of compounds as that obtained at this maximum. Knowing the corresponding transformation ratio (Table 7), it is possible to calculate the mass balance for complete kerogen degradation.

The next step is an addition of the mass balance from the first reaction to that of the second reaction, i.e. late generation of gas from the kerogen. In order to quantify separately this late gas potential, initial kerogens were pyrolysed either at 350°C/48 h or 375°C/15 h, conditions for which the oil pro-

Table 8. Late methane potential of the kerogens under study. C_{1r} is the amount of methane produced at 500°C/24 h by 1 g of the residual kerogen (kerogen 2) recovered either at 350°C/48 h or 375°C/15 h and C_l is the late methane potential for 1 g of carbon of the initial kerogen. The proportion of kerogen 2 is recalculated for TR = 100% in the first cracking reaction

Kerogen	C_{1r} (mg/g kerogen 2)	Kerogen 2 (wt% of the initial C)	C_l (mg/g C)
Type I	59	26	15
Type II	47	54	24
Type II-S	54	47	25
Type III Mahakam	51	77	39
Type III North Sea	56	80	45

duction is completed and all kerogen transformed into kerogen 2. The corresponding insoluble residues were recovered, extracted with dichloromethane and pyrolysed again under more severe conditions (500°C/24 h) during which gas production is completed (Table 8). It seems from these experiments that all kerogens 2, recovered after oil generation, have roughly the same gas potential C_{1r}. Knowing the percentage of kerogen 2 obtained previously for a TR of 100% in the first reaction, it is possible to estimate the late gas potential of each initial kerogen (C_l) by multiplying this percentage by the total amount of methane generated from the insoluble residue at 500°C/24 h. As this residual kerogen represents at least 77 wt% for the Type III samples, the contribution of the late gas generation to the total petroleum potential will be highest for this type of organic matter.

Combining the mass balances of the two reactions for closed system experiments, the resulting mass balance can be compared to that obtained in the open system, in mg/g of organic carbon in the initial kerogen (Table 9). Results show clear differences between the two pyrolysis systems: more methane and more NSOs are generated in closed system experiments whereas more wet gas and liquid hydrocarbons are produced in the open system. We had previously observed that in closed system pyrolysis, even for a TR below 60%, the absolute amounts of NSOs are greater than those obtained by Rock-Eval pyrolysis (TR = 100%). As we have recalculated the mass balance in the closed system for a TR of 100%, it is consistent to find higher yields for the NSO. Nevertheless, this difference suggests that a part of the NSOs is not quantified in the open system due to a less efficient extraction of these compounds from the pyrolysis chamber by the carrier gas as compared to solvent extraction. This leads to an underestimation of the total pyrolysate in the open system for the Type I, II and II-S samples. For the two coals, as their total pyrolysate is already underestimated in the closed system due to trapping, there is no significant difference in the HI in the two pyrolysis systems. The deficit in C_l for the open system could be related in part to the final temperature of the programmed pyrolysis not high enough to reach the end of methane generation (Behar *et al.*, 1995). However, another possible factor is the competition in the open system between hydrogen loss as methane or as molecular hydrogen. Whereas a very low hydrogen gas yield is observed in any of the experiments in the closed system, it has been shown (Behar *et al.*, 1995; Boudou and Espitalié, 1995) that for temperatures higher than 500°C in an open system, hydrogen gas production increases very rapidly.

It is possible to make a tentative evaluation of the amounts of gas and liquid hydrocarbons produced by secondary cracking of part of the NSOs in order to compare the open and closed systems. We have used the variations of mass balances in the closed system during NSO degradation and recalculated each fraction once the NSO amount is the same as that obtained in the open system. For the North Sea sample the C_l and C_2–C_5 analyses were not available in the selected pyrolysis experiment and the corresponding data on the Mahakam sample have been used. Although these calculations cannot be more than an estimate, it is a way of verifying our assumption for explaining the differences

Table 9. Comparison of the mass balances (mg/g C) calculated at TR = 100% for primary cracking of kerogen in open and closed pyrolysis systems; the total hydrogen index (HI) is the sum of C_l, C_2–C_5, C_6–C_{14} and C_{15+} fractions

Kerogen	Pyrolysis system	C_l	C_2–C_5	C_6–C_{14}	C_{15+} SAT	C_{15+} ARO	C_{15+} NSO	HI (mg/g C)
Type I	open	16	72	91	170	266	303	918
	closed	23	18	69	87	234	653	1083
Type II	open	19	50	54	33	134	310	600
	closed	32	14	20	23	130	496	715
Type II-S	open	26	44	83	29	151	227	560
	closed	32	6	74	19	120	497	748
Type III	open	31	24	23	14	17	85	194
Mahakam	closed	49	7	22	7	8	99	192
Type III North	open	31	26	17	10	26	102	212
Sea	closed	52	4	26	6	17	110	214

between the two systems. The resulting mass balances for closed and open systems, including both primary cracking and a similar contribution of secondary cracking of the NSOs, are compared in Fig. 3: although the resultant balances fit much better, there is a fairly systematic overestimation of hydrocarbons in the C_{6+} fraction, particularly in the C_6–C_{14} fraction. This could be attributed to the averaging of NSOs' hydrocarbon potential when using the closed system experiments, whereas the NSOs which are not swept away in the open system, being the heaviest, probably have a lesser hydrocarbon potential. However, these results show that, except for methane, there is no significant difference between open and closed system results at TR = 100% once the partial cracking of NSOs in the open system has been taken into account.

Kinetic parameters

Global optimization on the Rock-Eval S_2 peak (Optkin software). Kinetic parameters were derived using a parallel reaction model. The reactions of this kinetic scheme are considered to obey first-order kinetics and the Arrhenius law with various activation energies but a unique pre-exponential factor. The assumption of a unique pre-exponential factor is justified by the empirical need to reduce the number of free parameters rather than by theoretical considerations. Its practical effect is that elementary reactions occur in the order of increasing activation energies regardless of the temperature range (Tissot *et al.*, 1987). Discrete reactions, with a spacing of 1 or 2 kcal/mol between consecutive activation energies, were used. The optimization is achieved by minimizing an error function which is the sum of squared differences between experimental and model-computed S_2 peaks. Mathematical optimization is known to produce artefacts when the error function presents several close minima, a problem faced in the present situation for the pre-exponential factor. Recent improvements of the Optkin software enable a better search of the true minimum (Espitalié *et al.*, 1993). In addition, we have tried to get an independant check of this computed frequency factor by determining kinetic parameters on molecular tracers, as discussed later.

The distribution of the petroleum potential into four carbon classes for the five kerogens is shown in Fig. 4. The resulting kinetic parameters can be compared to those obtained by Tegelaar and Noble (1994) and authors cited therein. For the Type I kerogen primary cracking is described by one unique reaction with an activation energy at 54 kcal/mol and a frequency factor $A = 7.4 \times 10^{13}\ s^{-1}$, i.e. very close to the kinetic parameters cited elsewhere ($A = 1.8 \times 10^{14}\ s^{-1}$ and $E = 55$ kcal/mol in Tegelaar and Noble). For the Type II kerogen a broader distribution of reactions is observed with activation energies ranging mainly between 52 and 55 kcal/mol and a frequency factor $A = 1.6 \times 10^{14}\ s^{-1}$, also very close to the parameters given by Tegelaar and Noble for the Bakken Type II source rock ($A = 1.8 \times 10^{14}\ s^{-1}$ and $E = 53$–55 kcal/mol). As expected, liquid products appear very early for the Type II-S kerogen ($E = 46$–52 kcal/mol and $A = 2.5 \times 10^{13}\ s^{-1}$) whereas Tegelaar and Noble did not find such a large difference between Types II and II-S. However, these parameters are in good agreement with those of Pepper and Corvi (1995). In contrast to the Type I and II kerogens, very broad distributions of reactions are observed for the two coals and, although the composition of pyrolysates are different, the distributions of partial petroleum potentials for corresponding activation energies and the pre-exponential factors are very close ($A = 3 \times 10^{15}\ s^{-1}$ and $E = 56$–72 kcal/mol). The late methane generation is clearly observed above 60 kcal/mol and is completed for the North Sea sample only with the reaction at 74 kcal/mol.

Molecular tracers. Kinetic parameters obtained from pyrolysis experiments are used in basin modelling and thus extrapolated to geological conditions. A small difference in these parameters obtained under laboratory conditions can reach several orders of magnitude under natural conditions. It is thus important to cross-check the unique pre-exponential factor obtained by global kinetics with that measured on a single representative cracking reaction. The resulting compound, released by kerogen cracking, will be considered as a molecular tracer and should be abundant, easy to quantify and thermally stable once formed. Linear alkanes were selected as molecular tracers because they are abundant in crude oils and are well known to be the most thermally stable alkanes (Fabuss *et al.*, 1964). We studied the genesis of two individual *n*-alkanes C_{12} and C_{24}, which are found in all types of reservoir oils. For all the samples, except the Type II-S kerogen, it has been demonstrated already that the generation of *n*-C_{12} and *n*-C_{24} follows a first-order reaction (Tang and Behar, 1995; Behar *et al.*, 1997). Due to uncertainty in the determination of the rate constants, we estimated the activation energy calculations to be ± 1 kcal/mol. The resulting kinetic parameters for the five samples are given in Table 10.

Although the generation of *n*-C_{24} for the Type I, II and II-S samples is somewhat faster than that of the *n*-C_{12}, the activation energies and the frequency factors are fairly close to each other for a given kerogen type. Moreover, as expected, generation of the two *n*-alkanes is much faster for the Type II-S than for the Type I and II samples. These kinetic parameters for *n*-alkane generation in Type II-S are very close to those obtained from the same sample for pristene generation for which the activation energy and the frequency factor were respectively

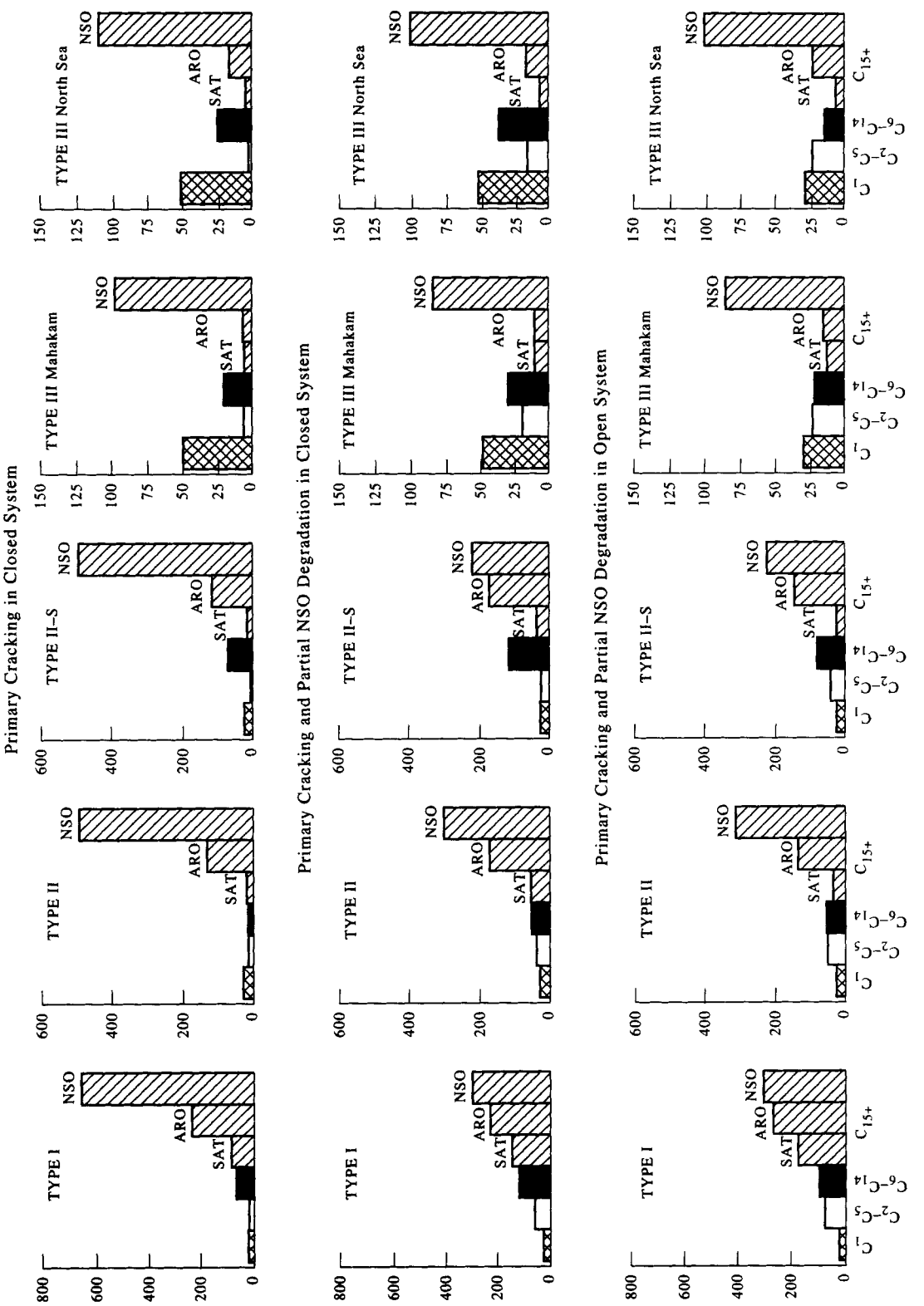

Fig. 3. Comparison of the mass balances recalculated for 100% TR in a closed system and same NSO degradation in open and closed systems.

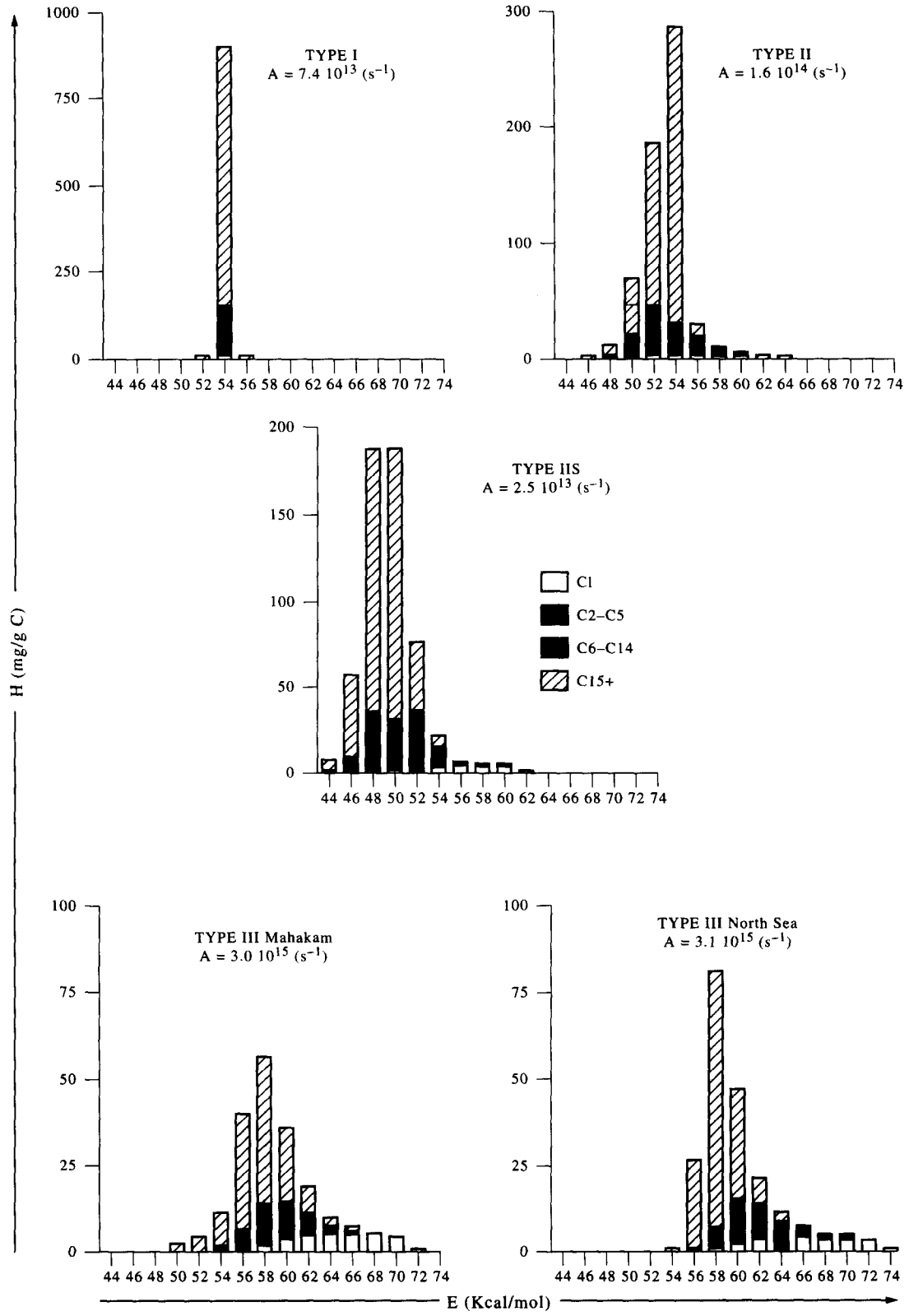

Fig. 4. Pre-exponential factors and kinetic distributions obtained by Optkin optimization on the compositional Rock-Eval pyrolysis data of the studied kerogens.

Table 10. Kinetic parameters (activation energy E and frequency factor A) obtained on molecular tracers n-C_{12} and n-C_{24} generated during primary cracking in open and closed systems under isothermal conditions

Kerogen	n-C_{12}		n-C_{24}	
	E (kcal/mol)	A (s^{-1})	E (kcal/mol)	A (s^{-1})
Type I	56.3	4.0×10^{14}	53.6	5.0×10^{13}
Type II	54.6	3.3×10^{14}	53.0	1.4×10^{14}
Type II-S	46.0	1.9×10^{11}	45.2	1.5×10^{11}
Type III Mahakam	55.5	2.9×10^{14}	46.1	6.4×10^{11}
Type III North Sea	57.8	8.1×10^{14}	48.9	3.3×10^{12}

46.1 kcal/mol and 1.9×10^{12} s^{-1} (Tang and Stauffer, 1995).

Kinetic parameters for n-C_{12} and n-C_{24} genesis from Type III samples are significantly different. In both samples the n-C_{24} activation energies and frequency factors are significantly lower than those obtained for n-C_{12}. This means that as far as n-alkanes are concerned very early generation of the heavy homologues occurs in Type III kerogens, as fast as for the Type II-S kerogen. It is worth noting that in recent work, Tang *et al.* (1996) have shown that the ratio between n-C_{16} and n-C_{30}, in a large number of coal extracts from various basins, increases dramatically with maturity. Our work on the thermal cracking of pure n-C_{25} (Behar and Vandenbroucke, 1996) shows that this n-alkane decomposes with an activation energy of 68.2 kcal/mole and a frequency factor of 6.1×10^{17} s^{-1}. When extrapolated to geological conditions, assuming, for instance, a sediment burial of 50 m per Myr and a geothermal gradient of 25°C/km, the n-alkanes window lies between 100 and 160°C for the Type III Mahakam coal, whereas the n-C_{25} starts to be cracked above 170°C. This suggests that the increase of the ratio n-C_{16} over n-C_{30} with maturation, in natural coal extracts, is not due to secondary cracking of n-C_{30} but to very different generation rates for light and heavy n-alkanes, probably due to breaking of different chemical bonds inside the coal structure. Similarly, some early generation of gas has also been predicted for coals by Tang *et al.* (1996), with a frequency factor of 9.9×10^{11} s^{-1} and activation energies ranging from 47 to 51 kcal/mol.

Kinetic parameters for molecular tracers such as n-alkanes or pristene can be compared to those obtained from global kinetics by compositional Rock-Eval pyrolysis (Table 2, Fig. 4 and Table 10). As Type I kerogen cracking was described with global kinetics by a single reaction (E = 54 kcal/mol and $A = 7.4 \times 10^{13}$ s^{-1}), it enables the two approaches to be directly cross-checked: the corresponding kinetic parameters are very close in both cases. Thus the molecular tracers, for which the reaction order and absolute kinetic parameters can be determined and then securely extrapolated from laboratory to geological conditions, are representative of the kerogen cracking kinetics. The advantage is that the uncertainty in the frequency factor and associated E due to optimization in global kinetics can be tested by that comparison. For Type II kerogen the frequency factor of global kinetics is also very close to that obtained using molecular tracers. For the Type II-S sample the frequency factor is slightly higher than those obtained either for the two n-alkanes or for pristene, and for the two Type III samples the frequency factors are so different by the two approaches that it is impossible to make a direct comparison without calculating the rate constants at a given temperature.

For all the samples we have thus compared the rate constants for various temperatures either in the range of laboratory (300–400°C) or geological (100–160°C) conditions. For global kinetics, we have selected the production of C_{15+} : knowing the proportion generated for each "slice" of activation energy (Table 2), it is possible to calculate an average activation energy and thus an average rate constant for a given temperature. The North Sea sample, being very similar to the Mahakam coal, has not been included in this calculation. For molecular tracers we have taken the kinetic parameters of the generation of n-C_{24} for Type I, II and III kerogens. For Type II-S kerogen, as kinetic parameters of pristene generation were available (Tang and Stauffer, 1995), we have taken an average activation energy for n-C_{24} and pristene (Pr) for calculation of the rate constants. These rate constants (in s^{-1}) calculated in the range of geological and laboratory temperatures, and the ratio (R) of the rate constants from global optimization over those from molecular tracers, are given in Table 11 and Fig. 5.

Our results show that for Type I, II and II-S samples the rate constants obtained with kinetic parameters from global optimization and from molecular tracers are very similar under both laboratory and geological conditions (Fig. 5). For the Type I sample the ratio varies from 1.1 to 1.0 under laboratory conditions whereas for the Type II-S kerogen, even if the pre-exponential factor is higher by global optimization, there is only an increase of R from 2.3 to 3.0 for the same temperature range, i.e. within the experimental error since we have estimated at 1 kcal/mol the uncertainty in the activation energy. For the

Table 11. Comparison of the rate constants obtained from global optimization and molecular tracers for laboratory (300–400°C) and geological (100–160°C) temperatures: *R* is the ratio between the rate constants from global kinetics and those of the molecular tracer

	Type I			Type II			Type II-S			Type III		
T (°C)	n-C_{24}	Global	*R*	n-C_{24}	Global	*R*	n-C_{24}/Pr	Global	*R*	n-C_{24}	Global	*R*
100	2.0×10^{-18}	1.7×10^{-18}	0.9	1.2×10^{-17}	2.3×10^{-17}	1.9	1.3×10^{-15}	9.8×10^{-16}	0.8	6.2×10^{-16}	1.8×10^{-18}	0.003
120	7.8×10^{-17}	6.9×10^{-17}	0.9	4.6×10^{-16}	8.3×10^{-16}	1.8	3.0×10^{-14}	2.7×10^{-14}	0.9	1.5×10^{-14}	8.6×10^{-17}	0.006
140	2.2×10^{-15}	2.0×10^{-15}	0.9	1.2×10^{-14}	2.1×10^{-14}	1.7	5.2×10^{-13}	5.3×10^{-13}	1.0	2.6×10^{-13}	2.8×10^{-15}	0.01
160	4.4×10^{-14}	4.1×10^{-14}	0.9	2.4×10^{-13}	4.0×10^{-13}	1.7	6.9×10^{-12}	7.9×10^{-12}	1.2	3.4×10^{-12}	6.6×10^{-14}	0.02
300	1.9×10^{-7}	1.7×10^{-7}	1.0	8.3×10^{-7}	1.2×10^{-7}	1.4	3.1×10^{-6}	7.1×10^{-6}	2.3	1.7×10^{-6}	5.9×10^{-7}	0.4
325	1.3×10^{-6}	1.4×10^{-6}	1.1	5.8×10^{-6}	7.9×10^{-6}	1.4	1.7×10^{-5}	4.2×10^{-5}	2.5	9.1×10^{-6}	4.6×10^{-6}	0.5
350	7.8×10^{-6}	8.4×10^{-6}	1.1	3.5×10^{-5}	4.6×10^{-5}	1.3	7.9×10^{-5}	2.1×10^{-4}	2.7	4.3×10^{-5}	3.1×10^{-5}	0.7
375	4.2×10^{-5}	4.6×10^{-5}	1.1	1.8×10^{-4}	2.4×10^{-4}	1.3	3.3×10^{-4}	9.6×10^{-4}	2.9	1.8×10^{-4}	1.8×10^{-4}	1.0
400	2.0×10^{-4}	2.2×10^{-4}	1.1	8.4×10^{-4}	1.1×10^{-4}	1.3	1.3×10^{-3}	3.9×10^{-3}	3.0	6.8×10^{-4}	9.3×10^{-4}	1.4

Type III samples, even in the laboratory, the rate constants start to diverge (R from 1.4 to 0.4) and under geological conditions R falls to 0.003. The differences observed for the kinetic parameters determined with the two approaches clearly demonstrate that when the distribution of reactions according to activation energies is very broad, it is questionable whether to maintain a constant frequency factor. Moreover, for Type III kerogen, the significant contribution of the late generation of gas, compared to oil, extends the reactions towards high activation energies. Consequently, the unique frequency factor found by optimization of the Rock-Eval S_2 peak may be, in fact, an average between a very low value around 10^{11} to 10^{12} s^{-1} for the early generation of paraffinic oil and a very high value around 10^{14} to 10^{15} s^{-1} for the late generation of gas.

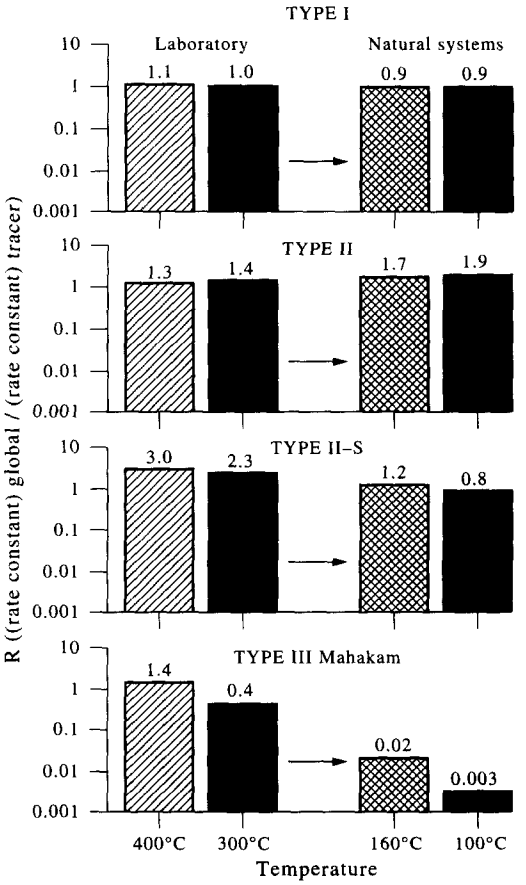

Fig. 5. Ratio of rate constants of kerogen degradation calculated with kinetic parameters from global kinetics and from molecular tracers in the temperature range of laboratory (400–300°C) and of geological systems (160–100°C). In Type I, Type II and Type II-S these ratios are in the same order of magnitude in the laboratory and in natural settings, whereas for Type III at 100°C rate constants calculated with global kinetics are three orders of magnitude lower than those obtained for n-C_{24} production.

CONCLUSIONS

Proposed strategy for determining kinetic parameters

Source rock typing. It is necessary to know the type and the evolutionary stage of the source rock organic matter before determining kinetic parameters for primary cracking. Sample typing can be done by pyrolysis–GC, preferably on the isolated kerogen but also on the source rock if its carbon content is high enough to avoid major cracking of the heavy compounds by matrix effect during pyrolysis (Behar and Pelet, 1984; Larter, 1984; Tegelaar and Noble, 1994; Curry, 1995). Typing analysis should be confirmed by optical characterization or elemental analysis of the isolated kerogen. Maturity of the sample can be determined by elemental analysis or Rock-Eval pyrolysis. However, vitrinite reflectance measurement should be a better maturity parameter for Type III organic matter. Hydrogen indices must be measured on the isolated organic matter in order to get the correct value for TR calculations. In fact, when the organic content of the source rock is low (< 2%), any experimental error on the total organic carbon can lead to a strong variation of the hydrogen index. Moreover, the presence of minerals may have side effects during pyrolysis.

Determination of kinetic parameters. For Type I, II and II-S kerogens the rate constants obtained either from global optimization or on molecular tracers are very similar. This indicates that the software used for optimization is able to search the correct minimum of the error function. This also validates the assumption of taking an unique frequency factor for all cracking reactions of a given sample. In terms of mass balances, the major difference between compositional Rock-Eval and closed system pyrolysis is the contribution of products generated from partial decomposition of the NSOs to primary products. As these compounds may be partly retained in source rocks (Sandvik *et al.*, 1991; Michelsen and Khorasani, 1995; Werner *et al.*, 1996), the mass balances obtained in open system pyrolysis could be more representative of those of fluids which are expelled from a source rock in the geological setting. Thus, for any new sample characterized as Type I, II or II-S kerogen, kinetic parameters can be determined using compositional Rock-Eval pyrolysis. As for typing, it is much better to work on isolated organic matter. The maturity stage of the studied sample must correspond to the very end of diagenesis, or the beginning of catagenesis, to obtain the entire set of oil potential distributions according to activation energies. Otherwise it is preferable to use default distributions for the corresponding source rock type. As a first step, one might run the optimization by fixing the frequency factor to that obtained on a reference sample, in order to see whether or not the distributions of activation energies are similar. If not, a specific optimization must be done for a search of another frequency factor value. In order to split the C_{15+} fraction into saturates, aromatics and NSOs, preparative pyrolysis is needed as various relative distributions of these compounds have been observed in the same type of organic matter. Each partial oil potential, by "slice" of activation energy, can then be split into six classes: C_1, C_2–C_5, C_6–C_{14}, C_{15+} saturates, C_{15+} aromatics and NSOs, assuming that the C_{15+} repartition is constant whatever the activation energy as shown by the reference samples. This fractionation enables a specific behavior to be assigned to petroleum compounds during migration: a part of the NSOs may not be expelled from the source rocks and thus can undergo secondary cracking together with the residual kerogen.

For Type III samples it is clearly not possible, in the non-isothermal open system, to optimize cracking reactions with a unique frequency factor for the complete distribution of activation energies: a very early generation of gas (Tang *et al.*, 1996) and liquids (Behar *et al.*, 1996) as well as a significant production of late gas occurs. At this stage of the present study it is difficult to propose default kinetic parameters for Type III samples. We suggest that attempts to fit partial Rock-Eval curves should be made. As a first step, as late gas generation seems to raise kinetic parameters to high values, we intend to optimize separately the C_1 and C_{2+} curves, obtained from Rock-Eval, with their own A and associated E values and to sum up the resulting amounts to reconstitute the total S_2 peak. The resultant A and E values should be nearer to those observed with molecular tracers, thus enabling a safer extrapolation to geological conditions. If the correlation between measured and calculated S_2 is good, better precision should be obtained by applying this procedure to each class separated by the compositional Rock-Eval. In terms of mass balance, as Type III organic matter has a high retention capability due to its tight structural network, a large proportion of generated products may not be expelled and will undergo secondary cracking. The composition of the expelled fluid is thus expected to be more similar to that obtained in compositional Rock-Eval pyrolysis than to that obtained in closed system pyrolysis (Table 9).

Late gas generation. A systematic underestimation of the late production of methane in compositional Rock-Eval pyrolysis is observed in comparison to that obtained in a closed system. This underestimation is partly due to too low a final temperature but also due to competitive formation of methane and molecular hydrogen, as shown by previous comparisons with TG–FTIR results (Behar *et al.*, 1995). We suggest that values of the open system should be corrected by those

obtained in the closed system for the reference samples. Artificial maturation studies on very mature kerogens in open and closed systems are currently in progress in order to specifically compare the mass balances and the kinetic parameters without taking into account the oil generation.

In conclusion, this study shows that at the present time compositional balances and kinetic parameters are reasonably similar when obtained by different pyrolysis techniques on reference Type I, II and II-S samples. The data obtained here can be used as default parameters for basin modelling. This is not the case for Type III organic matter. Further work is in progress to find a way to obtain kinetic parameters that may be extrapolated to geological conditions.

Associate Editor—**J. C. Hower**

Acknowledgements—O. Lerat, T. Lesage, D. Pillot and C. Sulzer are gratefully acknowledged for technical assistance. We also want to thank J. Burrus, A. Huc, A. Prinzhofer, J. L. Rudkiewicz and the two referees, M. Mastalerz and D. Taulbee, for their very helpful comments.

REFERENCES

Behar, F. and Pelet, R. (1984) Geochemistry of asphaltenes. *Organic Geochemistry* **6,** 587–595.

Behar, F. and Pelet, R. (1985) Pyrolysis–gas chromatography applied to organic geochemistry: structural similarities between kerogens and asphaltenes from related rock extracts and oils. *Journal of Analytical and Applied Pyrolysis* **8,** 173–187.

Behar, F. and Vandenbroucke, M. (1988) Characterization and quantification of saturates trapped inside kerogen network: implications for pyrolysate composition. *Organic Geochemistry* **13,** 927–938.

Behar, F. and Vandenbroucke, M. (1996) Experimental determination of the rate constants of the n-C_{25} thermal cracking at 120, 400 and 800 bar: implication for high pressure/high temperature prospects. *Energy and Fuels* **10,** 932–940.

Behar, F., Saint-Paul, C. and Leblond, C. (1989) Analyse quantitative des effluents de pyrolyse en milieu ouvert et fermé. *Revue de l'Institut Francais du Petrole* **44,** 387–397.

Behar, F., Kressmann, S., Rudkiewicz, J. L. and Vandenbroucke, M. (1991a) Experimental simulation in a confined system and kinetic modelling of kerogen and oil cracking. *Organic Geochemistry* **19,** 173–189.

Behar, F., Ungerer, P., Kressmann, S. and Rudkiewicz, J. L. (1991b) Thermal evolution of crude oils in sedimentary basins: experimental simulation in a confined system and kinetic modelling. *Revue de l'Institut Francais du Petrole* **46,** 151–181.

Behar, F., Vandenbroucke, M., Teermann, S. C., Hatcher, P. G., Leblond, C. and Lerat, O. (1995) Experimental simulation of gas generation from coals and a marine kerogen. *Chemical Geology* **126,** 247–260.

Behar, F., Tang, Y. and Liu, J. (1997) Comparison of rate constants for some molecular tracers generated during artificial maturation of kerogens: influence of kerogen type. *Organic Geochemistry* **26,** 281–287.

Boudou, J. P. and Espitalie, J. (1995) Molecular nitrogen from coal pyrolysis: kinetic modelling. *Chemical Geology* **126,** 319–333.

Burnham, A. and Braun, R. (1990) Development of a detailed model of petroleum formation, destruction and expulsion from lacustrine and marine source rocks. *Organic Geochemistry* **16,** 27–39.

Curry, D. J. (1995) The pyrolysis index: a rapid and reproducible technique for estimating the oil generation potential of coals and terrestrial kerogens. In *Organic Geochemistry: Developments and Applications to Energy, Climate, Environment and Human History*, eds. J. O. Grimalt and C. Dorronsoro, pp. 763–765. A.I.G.O.A., Spain.

Derbyshire, F., Marzec, A., Schulten, H.-R., Wilson, M. A., Davis, A., Tekel, Y. P., Delpuech, J. J., Jurkiewicz, A., Bronnimann, C. E., Wind, R. A., Maciel, G. E., Narayan, R., Bartle, K. and Snape, C. (1989) Molecular structure of coals: a debate. *Fuel* **68,** 1091–1106.

Durand, B. and Nicaise, G. (1980) Procedure for kerogen isolation. In *Kerogen*, ed. B. Durand, pp. 35–53. Editions Technip, Paris.

Espitalie, J., Senga Makadi, K. and Trichet, J. (1984) Role of mineral matrix during kerogen pyrolysis. *Organic Geochemistry* **6,** 365–382.

Espitalie, J., Ungerer, P., Irwin, I. and Marquis, F. (1988) Primary cracking of kerogens. Experimenting and modelling C_1, C_2–C_5, C_6–C_{15} and C_{15+} classes of hydrocarbons formed. *Organic Geochemistry* **13,** 893–899.

Espitalie, J., Marquis, F. and Drouet, S. (1993) Critical study of kinetic modelling parameters. In *Basin Modelling: Advances and Applications*, ed. A. G. Doré, pp. 233–242. NPF Special Publication 3, Elsevier, Amsterdam.

Fabuss, B. M., Smith, J. O. and Satterfield (1964) Thermal cracking of pure saturated hydrocarbons. In *Advances in Petroleum Chemistry and Refining*, ed. J. McKetta Jr. Vol. 5, pp. 156–201. John Wiley & Sons, New York.

Given, P. (1984) An essay on the organic geochemistry of coal. *Coal Science* **3,** 65–252.

Horsfield, B., Disko, U. and Leibtner, F. (1989) The micro-scale simulation of maturation: outline of a new technique and its potential application. *Geologische Rundschau* **78**(1), 361–374.

Larter, S. R. (1984) Application of analytical pyrolysis techniques to kerogen characterization and fossil fuel exploration/exploitation. In *Analytical Pyrolysis: Techniques and Applications*, ed. K. J. Voorhes, pp. 212–275. Butterworths, London.

Lewan, M. (1993) Laboratory simulation of petroleum formation: hydrous pyrolysis. In *Organic Geochemistry*, eds. M. H. Engel and S. A. Macko, Plenum Publishing Corporation, New York, pp. 419–422.

Michelsen, J. K. and Khorasani, G. K. (1995) The compositional differences related to the material balance of the expulsion dynamics, solid–fluid phase fractionation in the source rock and liquid–vapor phase fractionation during petroleum migration. In *Organic Geochemistry: Developments and Applications to Energy, Climate, Environment and Human History*, eds. J. O. Grimalt and C. Dorronsoro, pp. 275–277. A.I.G.O.A., Spain.

Monin, J. C., Connan, J., Oudin, J. L. and Durand, B. (1990) Quantitative and qualitative experimental approach of oil and gas generation: application to the North Sea source rocks. *Organic Geochemistry* **16,** 133–142.

Monthioux, M., Landais, P. and Monin, J. C. (1985) Comparison between natural and artificial maturation series of humic coals from the Mahakam delta. *Indonesian Journal of Organic Geochemistry* **8,** 275–292.

Pepper, A. S. and Corvi, P. J. (1995) Simple kinetic models of petroleum formation. Part 1: oil and gas generation from kerogen. *Marine and Petroleum Geology* **12,** 291–319.

Price, L. C. and Wenger, L. M. (1991) The influence of pressure on petroleum generation and maturation as suggested by aqueous pyrolysis. *Organic Geochemistry* **19,** 141–159.

Reynolds, J. G. and Burnham, A. K. (1993) Pyrolysis kinetics and maturation of coals from the San Juan basin. *Energy and Fuels* **7,** 610–619.

Sandvik, E. I., Young, W. A. and Curry, D. J. (1991) Expulsion from hydrocarbon sources: the role of organic absorption. *Organic Geochemistry* **19,** 77–87.

Serio, M. A., Hamblen, D. G., Markham, J. R. and Solomon, P. R. (1987) Kinetics of volatile product evolution in coal pyrolysis: experiment and theory. *Energy and Fuels* **1,** 138–152.

Solomon, P. R., Hamblen, D. G. and Carangelo, R. M. (1984) Analytical pyrolysis of coal using Ft–Ir. In *Analytical Pyrolysis: Techniques and Applications*, ed. K. J. Voorhees, pp. 121–158. Butterworths, London.

Tang, Y. and Behar, F. (1995) Rate constants of *n*-alkanes generation from Type II kerogen in open and closed pyrolysis systems. *Energy and Fuels* **9,** 507–512.

Tang, Y. and Stauffer, M. (1994a) Development of multiple cold trap pyrolysis. *Journal of Analytical and Applied Pyrolysis* **28,** 167–174.

Tang, Y. and Stauffer, M. (1994b) Multiple cold trap pyrolysis gas chromatography: a new technique for modeling hydrocarbon generation. *Organic Geochemistry* **22,** 863–872.

Tang, Y. C. and Stauffer, M. (1995) Formation of pristene, pristane and phytane: kinetic study by laboratory pyrolysis of Monterey source rock. *Organic Geochemistry* **23,** 451–460.

Tang, Y., Jenden, P. D., Nigrini, A. and Teerman, S. C. (1996) Modelling early methane generation. *Energy and Fuels* **10,** 659–671.

Teerman, S. C. and Hwang, R. J. (1991) Evaluation of the liquid hydrocarbon potential of coal by artificial maturation techniques. *Organic Geochemistry* **17,** 749–764.

Tegelaar, E. and Noble, R. A. (1994) Kinetics of hydrocarbon generation as a function of the molecular structure of kerogen as revealed by pyrolysis–gas chromatography. *Organic Geochemistry* **22,** 543–574.

Tissot, B. P., Pelet, R. and Ungerer, P. (1987) Thermal history of sedimentary basins, maturation indices and kinetics of oil and gas generation. *American Association of Petroleum Geologists* **71,** 1445–1466.

Tomic, J., Behar, F., Vandenbroucke, M. and Tang, Y. (1995) Artificial maturation of Monterey kerogen (Type II-S) in a closed system and comparison with Type II kerogen: implications on the fate of sulfur. *Organic Geochemistry* **23,** 647–660.

Ungerer, P. (1990) State of the art of research in kinetic modelling of oil formation and destruction. *Organic Geochemistry* **16,** 1–25.

Ungerer, P. and Pelet, R. (1987) Extrapolation of oil and gas formation from laboratory experiments to sedimentary basins. *Nature*, 327, 52–54.

Waples, D. W., Kamata, H. and Suizu, M. (1992) The art of maturity modeling. Part 1: Finding a satisfactory geological model. *American Association of Petroleum Geologists* **76,** 31–46; Part 2: Alternative models and sensitivity analysis. *American Association of Petroleum Geologists* **76,** 47–66.

Werner, A., Behar, F., de Hemptinne, J. C. and Behar, E. (1996) Thermodynamic properties of petroleum fluids during expulsion and migration from source rocks. *Organic Geochemistry* **24,** 1079-1095.